Volume 1 | Number 1 | Jan 2013 | Pages 1–100

RSC Advances

www.rsc.org/advances

ROYAL SOCIETY
OF **CHEMISTRY**

www.rsc.org/advances

Graphical abstract

for
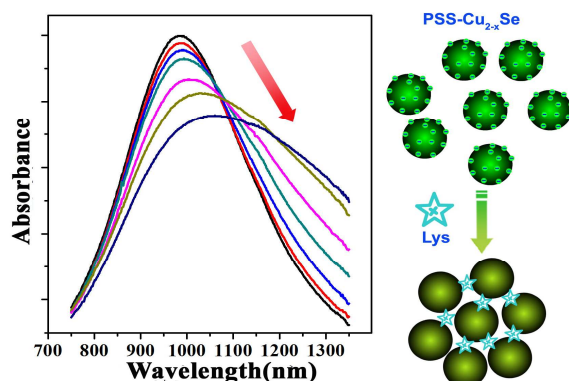
Tuning of the near-infrared localized surface plasmon resonance of $Cu_{2-x}Se$ nanoparticles with lysozyme-induced selective aggregation

Shao Qing Lie,[a] HongYan Zou,[b] Yong Chang,[a] and Cheng Zhi Huang*[a,b]

[a] Key Laboratory on Luminescence and Real-Time Analytical Chemistry (Southwest University), Ministry of Education, College of Chemistry and Chemical Engineering, Southwest University, Chongqing 400715, China

[b] College of Pharmaceutical Science, Southwest University, Chongqing 400716, China

Corresponding author: chengzhi@swu.edu.cn

Poly(styrene sulfonic acid)sodium stabilized $Cu_{2-x}Se$ nanoparticles (PSS-$Cu_{2-x}Se$ NPs) with localized surface plasmon resonance (LSPR) absorption centered at 980 nm can be selectively aggregated by lysozyme (Lys) through the electrostatic attraction, giving rise to a red shift of the LSPR in the near-infrared (NIR) region starting from 980 nm to 1300 nm area.

PAPER

Tuning of the near-infrared localized surface plasmon resonance of Cu₂₋ₓSe nanoparticles with lysozyme-induced selective aggregation

Shao Qing Lie,[a] Hong Yan Zou,[a] Yong Chang,[a] and Cheng Zhi Huang*[a,b]

In this paper, negatively charged $Cu_{2-x}Se$ nanoparticles (NPs) stabilized by poly(styrene sulfonic acid)sodium (PSS) (PSS-$Cu_{2-x}Se$ NPs) was synthesized via a simple templated method, which exhibited strong localized surface plasmon resonance (LSPR) absorption in the near-infrared (NIR) region. It was found that the prepared PSS-$Cu_{2-x}Se$ NPs could be aggregated by lysozyme (Lys) selectively through the

10 electrostatic interaction since the Lys was positively charged in neutral medium, producing a red shift of the LSPR band starting from 980 nm to 1300 nm area. With different concentration of Lys, the LSPR band can be dynamically tunned and the absorbance ratio of A_{1300}/A_{980} had a good linear relationship with the concentration of Lys in range of 5 nM~100 nM, supplying an effective way to tune LSPR in NIR region of semiconductor that might be applied for sensing and photothermal conversion sciences and

15 technologies in NIR region.

1. Introduction

More and more methods were established for evaluating optic systems, as well as for controlling some changes in the presence

20 of disturbances and parameter variations.[1, 2] Notably, some optic response exhibited by plasmonic nanostructures have been exploited and experimentally demonstrated.[3, 4] Therefore, plasmonic tune can be extensively applied in several fields, from surface-enhanced spectroscopies to biological and chemical

25 nanosensing.[5] Desirably, tuning the localized surface plasmon resonance (LSPR) offer more opportunities for controlling optical coupling into or out of nanoplasmonic devices or modulating plasmonic enhancement of spectroscopic signal.[6-9] Impressive efforts have been made in the synthesis of nanoparticles of noble

30 metals, such as Ag, Au, Cu and Pt, for the modulation of the plasmonic resonance.[10, 11] However, most chemical tuning of the plasmon is fixed at the end of their synthesis, which cannot generally be dynamically modified.

Recently, the heavily self-doped semiconductor materials

35 have received increasing attention for their dynamical plasmon in desired wavelength ranges which are not easily accessed by metal nanoparticles.[12-15] The berzelianite $Cu_{2-x}Se$, as a representive, is an important self-doped semiconductor with a relatively high carrier (holes) concentration and exhibits strong free carrier

40 absorption, which results in LSPR.[16] It is worthy to note that their LSPR tunability in a broad wavelength range can be controlled either by selecting crystal phase and composition in the preparation stage or by performing post synthesis red-ox and cation-exchange reactions.[16-18] For example, Dorfs et al.[18]

45 demonstrated that the infrared absorption of $Cu_{2-x}Se$ NCs could be tuned reversibly in the width and position by varying the

copper stoichiometry. Most of these LSPRs in copper chalcogenide nanocrystals depend on the tunable hole concentration induced by the copper deficiency,[16, 18, 19] and few

50 depend on surface or external conditions.

However, there has been theoretical and experimental researches on the plasmonic response to the surrounding medium, where the red-shift of NIR LSPR mostly depend on the increasing refractive index of the solvent.[17, 19] Moreover, the nanoparticles

55 coupling on the tunability of the LSPR band in the NIR has been also recently investigated,[17, 20] but few investigations take advantage of plasmonic coupling for biosensing, particularly the sensing in NIR regions, as comparable to the numerous reports concerning LSPR coupling arising in nanostructures of noble

60 metals as sensors.[21-23] In such sense, it is urgent to study more about NIR-LSPR coupling existed in vacancy-doped copper chalcogenide nanomaterials for a better understanding of the surrounding effect on the NIR-LSPR.

Herein, we report a biomacromolecule induced selective

65 aggregation of $Cu_{2-x}Se$ NPs that can make a strong coupling action to regulate the NIR LSPR, creating new opportunities for plasmonic manipulation of light and investigation into light−matter interactions at the nanoscale. We demonstrate for the first time that lysozyme (Lys), an important enzyme which is

70 widely distributed in body tissues and secretions,[24] induced the aggregation of $Cu_{2-x}Se$ NPs capped by poly(styrene sulfonic acid)sodium (PSS-$Cu_{2-x}Se$ NPs) (Scheme 1). Owing to the electrostatic interaction, the Lys can easily induce the aggregation of PSS-$Cu_{2-x}Se$ NPs with negative charge in neutral medium as

75 the Lys was positively charged with a high p*I* (p*I*=11.0). With the aggregation of the PSS-$Cu_{2-x}Se$ NPs, the NIR-LSPR absorption shifts to long wavelength, making it easy and low-cost to tune the

LSPR in the infrared range where the solar spectrum has the maximum photon fluence, in contrast to noble metal nanoparticles in the blue part of the spectrum.[25, 26]
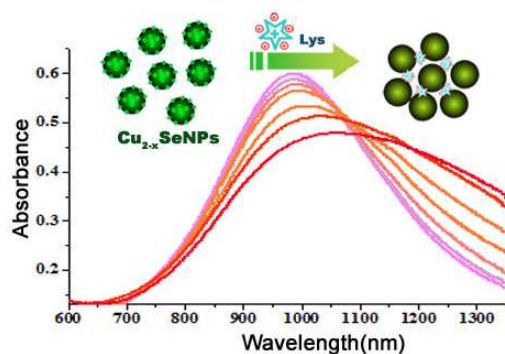
Scheme 1. Schematic illustration of the aggregation of PSS-Cu$_{2-x}$Se induced by Lys.

2. Experimental Section

2.1 Reagents

Lys and trypsin were bought from Sigma-Aldrich Co. LLC. (St. Louis. MO. USA). Thrombin was purchased from Haematologic Technologies Inc. (USA). Pepsin was from Shanghai Biochemicals (Shanghai, PRC). Helicase and cellulose were both commercially obtained from Beijing BioDev-Tech. Scientific&Technical Co. Ltd.. Copper sulfate (CuSO$_4$·5H$_2$O, 99%) and sodium chloride (NaCl) were purchased from Sinopharm Chemical Reagent Co., Ltd. (Shanghai, China). Stock solution of proteins including Lys (1 mM) was prepared and diluted in deionized water as necessary. Selenious dioxide (SeO$_2$, 99.9%) was obtained from Aladdin Chemistry Co., Ltd. (Shanghai, China). Ascorbic acid (Vc) and poly(styrene sulfonic acid)sodium (PSS, MW 70 kD) were purchased from Alfa Aesar Co., Ltd. (MA, USA). 20 mM PB buffer was prepared with sodium phosphate dibasic dodecahydrate and sodium phosphate monobasic dehydrate used in our experiments. All chemicals were used as received without further purification and dissolved in doubly distilled water (18.2 MΩ).

2.2 Instruments

The absorption spectra were measured with an U-3600 spectrophotometer (Hitachi Ltd., Japan). Light scattering spectra were recorded by synchronous scanning with F-4500 fluorescence spectrophotometer (Hitachi, Japan). S-4800 scanning electron microscope (SEM) (Hitachi, Japan) and transmission electron microscope (TEM) (JEM-2100, Japan) were used for imaging the size and shape of Cu$_{2-x}$Se NPs. Zeta potential values and the average hydrodynamic diameters of Cu$_{2-x}$Se NPs were measured with a Zetasizer Nano ZS/ZEN3600 (Malvern Instruments, Malvern, UK).

2.3 Preparation of Cu$_{2-x}$Se NPs

The PSS-Cu$_{2-x}$Se NPs were prepared by a simple templated method.[27] Briefly, 1.6 ml 10 mg/ml PSS and 5.5 ml water were added to a round-bottom flask and then 0.1 ml 0.2 M SeO$_2$ and 0.3 ml 0.4 M Vc were added, successively. After 10 min, a mixed solution of 0.1 ml 0.4 M CuSO$_4$·5H$_2$O and 0.4 ml 0.4 M Vc was added under vigorous stirring. The resulting mixture was allowed to proceed under vigorous stirring at room temperature in 10 h until a green solution was obtained and purified through a 10 kDa dialysis membrane for 1 day with 6 changes of distilled water. After the dialysis, PSS-Cu$_{2-x}$Se was centrifugated at 10000 rpm for 10 min to remove excess PSS. The product was stored in 4°C fridge and kept for the application.

### 2.4 UV-vis-NIR and scattering spectrometric measurement

The UV-vis-NIR absorption spectra with the wavelength range from 300 nm to 1350 nm and absorbance values at 980 nm (A_{980}) and 1300 nm (A_{1300}) were measured. The ratio of A_{1300}/A_{980} in both the presence (A) and absence (A_0) of Lys were recorded to identifiy the aggregation of PSS-Cu$_{2-x}$Se NPs. The light scattering spectra (the wavelength range from 200 to 700 nm) and values at 500 nm (I_{500}) and 350 nm (I_{350}) were also measured by simultaneously scanning the excitation and emission monochromators of the spectrofluorometer with $\lambda_{em} = \lambda_{ex}$.

2.5 Interaction between Lys and Cu$_{2-x}$Se NPs

Different concentrations of Lys were added to a solution of PSS-Cu$_{2-x}$Se, 75 mM NaCl, and 20 mM PB buffer, in which the concentration of PSS-Cu$_{2-x}$Se was about 0.1 nM with absorbance at 980 nm being about 0.6. The resulting mixture was equilibrated for the optimal incubation time before measurement.

3. Results and discussion

3.1 Characterization of PSS-Cu$_{2-x}$Se NPs
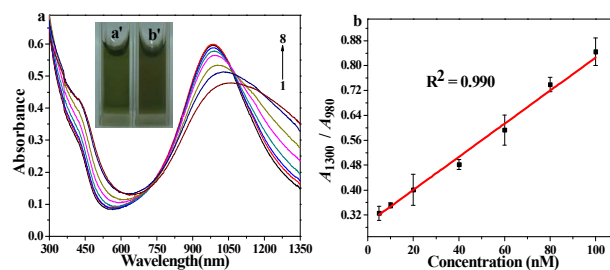
Fig. 1 Changes of the absorption upon the addition of Lys. (a) UV-vis-NIR absorption spectra of the PSS-Cu$_{2-x}$Se NPs in the presence of different concentration of Lys, from 1 to 8 (nM): 0, 5, 10, 20, 40, 60, 80, 100. The inset shows the corresponding color of the solution in the absence (a') and presence (b') of 60 nM Lys. (b) The plot of A_{1300}/A_{980} ratios of the PSS-Cu$_{2-x}$Se NPs as a function of the Lys concentration. 20 mM phosphate buffer solution containing 75 mM NaCl were used, pH 8.0.

As shown in Fig. 1a, a green colloidal dispersion of PSS-Cu$_{2-x}$Se NPs exhibited an intensive absorption band extended from 300 nm to 1350 nm with a strong characterisitc peak at 980 nm. The NIR absorption is assigned to NIR LSPR,[16] which suggests a relatively high concentration of free carriers.[27] From TEM and high-resolution TEM (HRTEM) (Fig. 2) measurements, the prepared Cu$_{2-x}$Se NPs has an average diameter at about 40 nm and lattices of (111) crystal planes with a 0.330 nm interplane-distance.[28] The corresponding indexed fast Fourier transforms (FFTs, Fig. 2c) of the lattice resolved image was indexed to the cubic structure of Cu$_{2-x}$Se with the zone axes along the direction of (011), indicating that the nanoparticles were well-crystallized. The selected area electron diffraction (SAED) pattern (Fig. 2d)

also showed the cubic crystalline structure of berzelianite with several rings indexed to the (111), (200), (220), and (311) planes.[29] Furthermore, the nanoparticles exhibited excellent stability in aqueous solutions, even in the presence of high concentration of salt, so that the PSS-Cu_{2-x}Se NPs could be stable in a high ionic strength medium of 100 mM NaCl, wherein NaCl neutralize the charge of PSS-Cu_{2-x}Se NPs from -60 mV to -32.3 mV which did not make any change of the spectra.
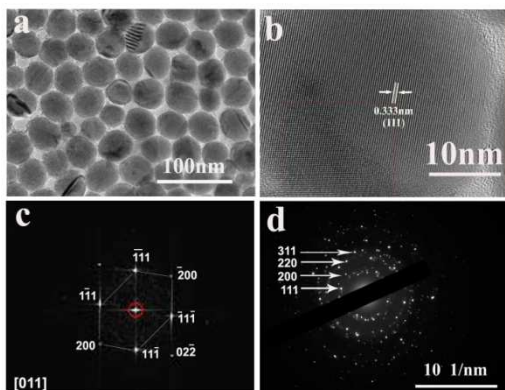
Fig. 2 The images showing the crystalline of PSS-Cu_{2-x}Se NPs. (a) TEM, (b) HRTEM image, (c) FFTs and (d) SAED spectrum.

3.2 The interaction between PSS-Cu_{2-x}Se NPs and Lys

With the addition of Lys to PSS-Cu_{2-x}Se NPs solution, the absorption of the colloidal solution gets broadened with a shift to long wavelength at the price of the absorption at 980 nm (Fig. 1a), giving rise to a slight change of the colour, which was consistent with the monotonically rising absorption at wavelengths below 500 nm in presence of Lys. With increasing the Lys concentration (from 5 to 100 nM), the absorption of the PSS-Cu_{2-x}Se NPs solution gets decreased at 980 nm and increased at 1300 nm gradually, showing a good linear relationship of the absorption ratios (A_{1300}/A_{980}) against the Lys concentration in the ranges from 5 nM to 100 nM with a correlation coefficients (R^2) of 0.99 (Fig. 1b).

In order to study the changes in the light absorption features, the average hydrodynamic diameters and SEM images of Cu_{2-x}Se NPs solutions were measured (Fig. 3). DLS measurements, which could well reflect the size changes, showed that the particle sizes of the PSS-Cu_{2-x}Se NPs got increased with increasing Lys concentration (Fig. 3a). As the SEM images shown (Fig. 3b, c, d), the addition of Lys has induced state change of PSS-Cu_{2-x}Se NPs from dispersion to aggregation. The shift of LSPR band was mostly interpreted as quantum size effects.[19] But here pronounced size quantization effects was not observed because of the large dimensions (>10 nm in diameter) compared to the estimated Bohr radius (3-5 nm). As shown in Fig. 4, the light scattering features show the rayleigh scattering signals of Cu_{2-x}Se NPs, which are related to their size and environments. Corresponding to DLS measurements, the light scattering get proportionally increased with increasing the concentration of Lys, where characteristic peaks at 350 nm and 500 nm get obviously changed.

Therefore, we can conclude that the NIR LSPR changes of PSS-Cu_{2-x}Se NPs with the addition of Lys were due to the close packing of nanoparticles which may result in a well studied phenomenon of LSP coupling. In such case, the aggregation-

induced LSPR tuning in NIR suggests opportunities in structures active at telecommunication wavelengths.
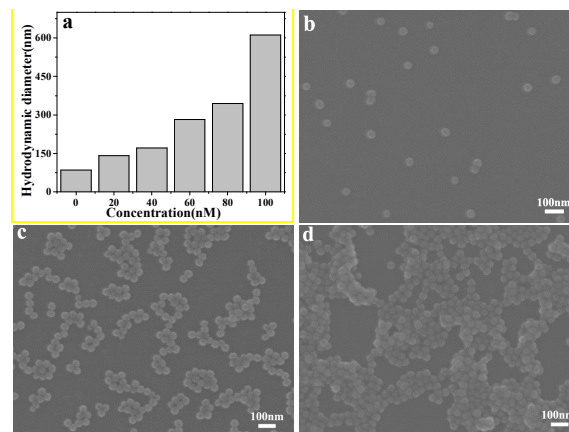
Fig. 3 Lys-induced aggregation of PSS-Cu_{2-x}Se NP. DLS measurements (a) and SEM images (b, c, d) showing the aggregation of PSS-Cu_{2-x}Se NPs in the presence of Lys. Concentration of Lys in SEM imaging (nM): b, 0; c, 20; d, 100.
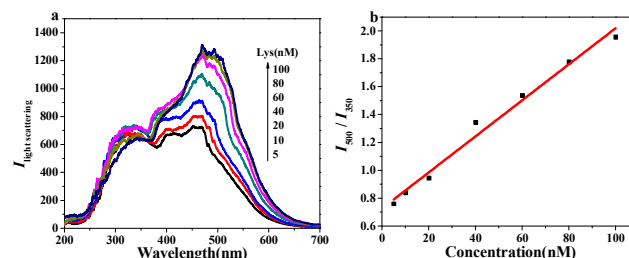

Fig. 4 Light scattering features changes of the PSS-Cu_{2-x}SeNPs upon the addition of Lys. (a) Light scattering enhanced with the increasing concentration of Lys within the range of 5-100 nM. (b) The plot of I_{500}/I_{350} ratios of the PSS-Cu_{2-x}Se NPs as a function of the Lys concentration. Buffer: 20 mM phosphate solution containing 75 mM NaCl, pH 8.0.

3.3 The mechanism of tuning LSPR with Lys

As shown in Fig. 1a, the addition of Lys cause an intresting red-shift of the NIR LSPR and a noticeable broadening of the LSPR band. In addition, the red-shift of max wavelength (λ_{max}) get increased exponentially with the concentration of Lys (Fig. 5a). The Lys-induced aggregtion results in the decreased distance between neighboring nanoparticles, accompanied with the increased strength of near-field coupling interactions.[30] Here it is found the state change from the aggreagtion to dispersion when the concentration of Lys is over 100 nM, so we defined the 100% aggregation when 100 nM Lys. Different from previous report wherein LSPR are mostly based on the tunable hole concentration induced by the copper vacancies in copper chalcogenide nanocrystals,[17, 18] herein we tune the LSPR feature by changing the degree of close-packing neighbouring nanoparticles. It is assumed that such coupling also influence the carrier concentration, which could be estimated by caculating the different absorption peak of PSS-Cu_{2-x}Se NPs in presence of Lys using the Maxwell Garnett effective medium theory and the Drude model. [31]

From the SEM of PSS-Cu_{2-x}Se NPs in presence of Lys, it is clear that the particles are close enough for their near-field to interact, so the collective properties of the whole ensemble contribute to the optical properties. And the small particle clusters
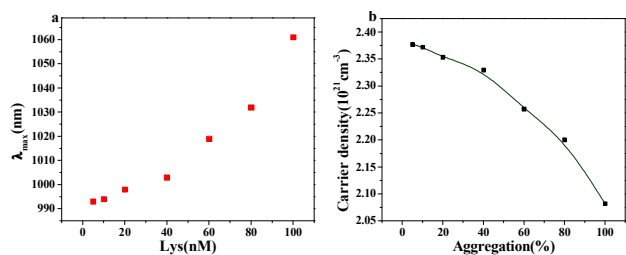
Fig. 5 The tuning of NIR LSPR with Lys. (a) The red-shift of the NIR LSPR wavelength (λ_{max}) with the increasing of Lys. (b) The decreasing of carrier density in the PSS-Cu$_{2-x}$SeNPs with the increased degree of aggregation. The degree of aggregation is estimated to be 100% induced by 100 nM of the Lys. Buffer: 20 mM phosphate solution containing 75 mM NaCl, pH 8.0.

in solutions to the effective dielectric function of such material ε_{eff} as[31]

$$\varepsilon_{eff} = \varepsilon_m \frac{\varepsilon(1+2f) + \varepsilon_m(1-f)}{\varepsilon(1-f) + \varepsilon_m(2+f)} \quad (1)$$

wherein f is the filling factor introduced to describe the topology as:

$$f = \frac{V_{cluster}}{V_{sample}} \quad (2)$$

From the DLS of PSS-Cu$_{2-x}$Se NPs with 100 nM of Lys, the aggreate of the PSS-Cu$_{2-x}$Se NPs reach a maxium diameter of 600 nm (r<λ_{max}). Assuming the aggregate to be spherical, a simple functional form of the filling factor can be given by

$$f = \frac{NR^3}{r^3} \quad (3)$$

where r is the radius of the spherical aggregate,R is the radius of the spherical NCs, and N is the number of the particles in the system. According to the Drude model,[19] the bulk plasma frequency ω_p highly depends on the density of free carriers (holes) as

$$\omega_p = \sqrt{\frac{N_h e^2}{\varepsilon_0 m_h}} \quad (4)$$

wherein N_h is the free hole density, e is the electron charge, ε_0 is the free space permittivity, and m_h is the hole effective mass, approximated as $0.4\ m_0$ where m_0 is the electron mass.[19]

To estimate changes in the carrier density assuming negligible interparticle interactions, there is only one resonance at $\varepsilon = -2\varepsilon_m$ corresponding to the surface plasmon resonance at $\omega = \omega_p/(1+\varepsilon_m)^{1/2}$ of the particle clusters. Therefore, the density of free carriers (holes) N_h can be calculated (Fig. 5b), which decrease with the increasing aggregation of NPs. It is expected that the increasing aggregation of NPs induce stronger light scattering and stronger near-field interaction.[20] As the sample absorption (A) is expressed by the formula A=1-(T+S), where T is the transmitted and S the scattered light from the sample, the increase of scattered light resulted in an obvious incresing of absorption in the visible region (Fig. 1a). The tune of absorption in near infrared region should be attributed to the strong electric field effects, which suggests the strong near-field interaction may affect the concentration of free carriers. Therefore, the broadening and the decreasd intesity of LSPR can be attributed to

the effect of electric field interaction.[30] Recent reports have demonstrated the non interacting NCs show weak nearfield enhancement factors[32] and near-field coupling is highly dependent on carrier density, showing weak near-field coupling in assemblies of Cu sulfide nanodisks with moderate carrier densities.[20] However, for the prepared Cu$_{2-x}$Se NPs with lower hole effective mass of 0.4 m_0 than the reported Cu sulfide nanodisks, it is suggested that a relatively strong near-field coupling exsited in the aggregation resulting in a red-shift of the LSPR band.
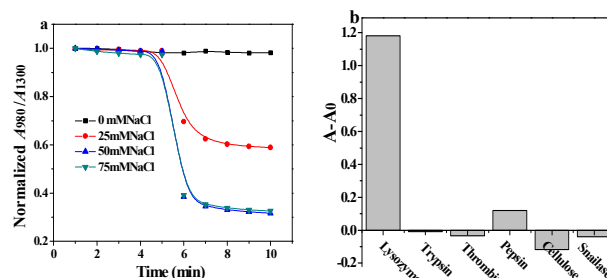
Fig. 6 Effects on tuning the LSPR. (a) Changes in the LSPR peaks of PSS-Cu$_{2-x}$Se NPs with time increasing upon the addition of 60 nM Lys in different concentration of NaCl. (b) The selective tuning by comparing 100 nM trypsin, 100 nM thrombin, 100 nM pepsin, 100 nM cellulose and 60 nM lysozyme.

It was found that the ionic strength could also influence the aggregation of PSS-Cu$_{2-x}$Se NPs by Lys. Higher ionic concentration caused larger change of absorption with increasing incubation time (Fig. 6a). Without any NaCl added, the absorption spectra had no change even in presence of Lys. With increasing the ionic concentration, the LSPR get increasing degree of modulation. 75 mM NaCl results in a remarkable change of the surface plasmon resonance band which identified it an appropriate ionic strength to promote the interaction of PSS-Cu$_{2-x}$Se NPs and Lys. The interaction of PSS-Cu$_{2-x}$Se NPs and Lys was very fast within 10 min as the aggregation was driven by the London/vander Waals attractive force between the nanoparticles.[25] Once the electrostatic repulsion was significantly reduced due to the loss (or screen) of surface charges, the attractive forces dominate, leading to a rapid aggregation.[33] This was further confirmed by surface charge measurements: the zeta potentials of PSS-Cu$_{2-x}$Se NPs in the absence of and presence of Lys were -64.6 ± 2 mV and -30.6 ± 1 mV, respectively. However, it is the strong interacting between NPs that cause the change of LSPR instead of the surface charge. Besides, it has been found that other proteins, including trypsin, thrombin, pepsin, cellulose and snailase all with concentrations of 100 nM induce no obvious change in the absorption of PSS-Cu$_{2-x}$Se NPs compared to 60 nM Lys (Fig. 6b), so Lys can induce a selective regulation of the NIR LSPR.

4. Conclusions

In conclusion, we developed a new strategy to tune LSPR of Cu$_{2-x}$Se NPs which can be used as plasmonic sensor for the detection of Lys at nanomolar level. The aggregation of PSS-stabilized Cu$_{2-x}$Se NPs induced by Lys produced an obvious absorption change and enhanced light scattering, as well as influenced the hole concentration. This method indicated the LSPR was very sensitive to the coupling of PSS-Cu$_{2-x}$Se NPs. Meanwhile, the

value of this proposed method lies in the simplicity and high sensitivity that are consistent with the resources and needs of many laboratories. Furthermore, this proposed method can be extended to the detection of any other analytes of interest using the low-cost $Cu_{2-x}Se$ NPs as an LSPR sensor, thus will be expected to see more applications of $Cu_{2-x}Se$ NPs with strong NIR-LSPR.

Acknowledgements

Notes and references

[a] *Education Ministry Key Laboratory on Luminescence and Real-Time Analysis, School of Chemistry and Chemical Engineering, Southwest University, Chongqing 400715, China. E-mail: chengzhi@swu.edu.cn, Tel: (+86) 23 68254659, Fax: (+86) 23 68367257.*
[b] *College of Pharmaceutical Science, Southwest University, Chongqing 400716, China*

1 J.-J. E. Slotine, *Int. J. Control*, 1984, **40**, 421-434.
2 C. Zhang, Y. Song and X. Wang, *Coordin. Chem. Rev.*, 2007, **251**, 111-141.
3 K. F. MacDonald, Z. L. Samson, M. I. Stockman and N. I. Zheludev, *Nat. Photon.*, 2009, **3**, 55-58.
4 M. Kauranen and A. V. Zayats, *Nat Photon*, 2012, **6**, 737-748.
5 I. S. Mark, *New J. Phys.*, 2008, **10**, 025031.
6 G. Garcia, R. Buonsanti, E. L. Runnerstrom, R. J. Mendelsberg, A. Llordes, A. Anders, T. J. Richardson and D. J. Milliron, *Nano Lett.*, 2011, **11**, 4415-4420.
7 H. Chen, R. Li, H. Li and J.-M. Lin, *J. Phys. Chem. C*, 2012, **116**, 14796-14803.
8 H. Chen, W. Xue, C. Lu, H.-f. Li, Y. Zheng and J.-M. Lin, *Spectrochim. Acta. Part A*, 2013, **116**, 355-360.
9 H. Chen, L. Lin, H. Li and J.-M. Lin, *Coordin. Chem. Rev.*, 2014, **263–264**, 86-100.
10 K. L. Kelly, E. Coronado, L. L. Zhao and G. C. Schatz, *J. Phys. Chem. B*, 2002, **107**, 668-677.
11 K.-S. Lee and M. A. El-Sayed, *J. Phys. Chem. B*, 2006, **110**, 19220-19225.
12 Y. Zhao and C. Burda, *Energy Environ. Sci.*, 2012, **5**, 5564-5576.
13 A. L. Routzahn, S. L. White, L.-K. Fong and P. K. Jain, *Isr. J. Chem.*, 2012, **52**, 983-991.
14 F. Scotognella, G. Valle, A. Srimath Kandada, M. Zavelani-Rossi, S. Longhi, G. Lanzani and F. Tassone, *Eur. Phys. J. B*, 2013, **86**, 1-13.
15 A. Comin and L. Manna, *Chem. Soc. Rev.*, 2014, **43**, 3957-3975.
16 Y. Zhao, H. Pan, Y. Lou, X. Qiu, J. Zhu and C. Burda, *J. Am. Chem. Soc.*, 2009, **131**, 4253-4261.
17 I. Kriegel, C. Y. Jiang, J. Rodriguez-Fernandez, R. D. Schaller, D. V. Talapin, E. da Como and J. Feldmann, *J. Am. Chem. Soc.*, 2012, **134**, 1583-1590.
18 D. Dorfs, T. Härtling, K. Miszta, N. C. Bigall, M. R. Kim, A. Genovese, A. Falqui, M. Povia and L. Manna, *J. Am. Chem. Soc.*, 2011, **133**, 11175-11180.
19 J. M. Luther, P. K. Jain, T. Ewers and A. P. Alivisatos, *Nat. Mater.*, 2011, **10**, 361-366.
20 S.-W. Hsu, C. Ngo and A. R. Tao, *Nano Letters*, 2014, **14**, 2372-2380.
21 J. N. Anker, W. P. Hall, O. Lyandres, N. C. Shah, J. Zhao and R. P. Van Duyne, *Nat. Mater.*, 2008, **7**, 442-453.
22 H. Li and L. Rothberg, *Proc. Natl. Acad. Sci. USA*, 2004, **101**, 14036-14039.
23 H. Zheng, S. Qiu, K. Xu, L. Luo, Y. Song, Z. Lin, L. Guo, B. Qiu and G. Chen, *Analyst*, 2013, **138**, 6517-6522.
24 Z. Yu, Q. Meng, H. Yu, B. Fan, S. Yu, J. Fei, L. Wang, Y. Dai and N. Li, *J. Dairy Sci.*, 2006, **89**, 2911-2918.
25 C.-J. Y. Yi-Ming Chen, Tian-Lu Cheng, and Wei-Lung Tseng, *Langmuir* 2008, **24**, 3654-3660.
26 X. Wang, Y. Xu, Y. Chen, L. Li, F. Liu and N. Li, *Anal. Bioanal. Chem.*, 2011, **400**, 2085-2091.
27 S. Q. Lie, D. M. Wang, M. X. Gao and C. Z. Huang, *Nanoscale*, 2014, **6**, 10289-10296.
28 J. Choi, N. Kang, H. Y. Yang, H. J. Kim and S. U. Son, *Chem. Mater.*, 2010, **22**, 3586-3588.
29 Z. Deng, M. Mansuripur and A. J. Muscat, *J. Mater. Chem.*, 2009, **19**, 6201-6206.
30 I. Kriegel, J. Rodríguez-Fernández, E. D. Como, A. A. Lutich, J. M. Szeifert and J. Feldmann, *Chem. Mater.*, 2011, **23**, 1830-1834.
31 S. K. Ghosh and T. Pal, *Chem. Rev.*, 2007, **107**, 4797-4862.
32 I. Kriegel, J. Rodriguez-Fernandez, A. Wisnet, H. Zhang, C. Waurisch, A. Eychmuller, A. Dubavik, A. O. Govorov and J. Feldmann, *ACS Nano*, 2013, **7**, 4367-4377.
33 K. Sato, K. Hosokawa and M. Maeda, *J. Am. Chem. Soc.*, 2003, **125**, 8102-8103.